International Conference on Renewable Energies and Power Quality (ICREPQ'16)
Madrid (Spain), 4th to 6th May, 2016
Renewable Energy and Power Quality Journal (RE&PQJ)
ISSN 2172-038 X, No.14 May 2016

Power Factor Corrector Design applied to an 85-kHz Wireless Charger

J.M. González-González, D. Fernández Cabrera, A. Triviño, J. A. Aguado

Department of Electrical Engineering
University of Málaga
Málaga (Spain)
josemanuelgonzalez@uma.es

***Abstract*—Wireless charging technology extends the battery autonomy by allowing more flexible and practical ways of recharging it even when the electric vehicle is on move. The frequency conversion, which is required to generate a kHz-ranged magnetic field, also leads to considerable harmonics. As a result, the power factor and the corresponding efficiency decrement. This paper proposes a Power Factor Corrector which overcomes this drawback. The most relevant feature of the designed Power Factor Corrector is that it does not need any electrical signal from the secondary side to adjust its operation properly. The simulation results show the ability of the proposed scheme to increment the system efficiency for different State-Of-Charge in the Battery.**

***Keywords*—Electric Vehicle, Power Factor Corrector, Primary control, Wireless Charger.**

I. INTRODUCTION

Wireless chargers provide the flexibility to charge the EVs (Electric Vehicles) without the need for any physical contact or even user's intervention [1]. This is a quite relevant advantage that allows EV to be charged on move. As a consequence, wireless chargers are able to extend vehicle's autonomy.

The behavior of a wireless charger or ICPT (Inductively-Coupled Power Transfer) relies on the generation of a magnetic field. Indeed, the main structure in a wireless charger is composed of two coupled coils. The coil in the pavement (also referred as the primary coil) is excited with an alternating current so that a voltage is induced in the coil placed in the vehicle (usually named as secondary coil). Aiming at reaching a maximum power transfer, both coils are equipped with adjacent reactive structures [2].

Additionally, the current in the primary is set in the HF (High Frequency) range so that conveniently sized coils can be utilized. Thus, power converters are demanded to enable the frequency conversion from the grid to the one used for the magnetic field. Specifically, a rectifier-inverter topology is usually installed in the primary. However, this inclusion leads to a degradation of the system efficiency. Particularly, multiple harmonics appear in the current sourced from the grid and, in turn, the real power provided by the utility decrements. This impact is modeled by the diminution of the power factor.

In order to overcome this limitation, PFCs (Power Factor Corrector) techniques need to be considered [3]. Power Factor Corrector schemes aims at generating an in-phase sinusoidal current in the source. When applied to a wireless charger, this capability must be guaranteed even for different battery states, that is, for a range of load values.

For single-phase wireless charger, two approaches may be followed for using a PFC. They differ on the power converter that is altered to get a power factor similar to the unity. Firstly, PFC can be included in the control algorithm belonging to the inverter so that the generated switching signals are able to modify the power factor [4]. As a second option, PFC may be integrated between the rectifier and the inverter in the primary side [5]. In both works, the PFC adjustment is achieved by forcing operating frequencies different to the resonant one. The main limitation of these proposals relies on the fact that they demand feedback signals from the secondary side to operate their control structures. Obtaining these signals may not be straightforward. Being opposite to the ICPT paradigm, a wired connection is not recommended. Alternatively, a wireless transmission system could be included towards this goal. In this way, more error-prone components are in the wireless charger and a wireless protocol needs to be configured in a receptor in the primary side and in a transmitter in the secondary side.

Our present work avoids feedback signals from the secondary side. The designed wireless charger is able to simultaneously control the power factor and the power delivered to the battery. Both controls are placed in the primary side. Particularly, we have incorporated a PFC between the rectifier and the inverter in the primary side as in [5]. The PFC controls the current waveform in the utility by means of local signals. In addition, the inverter adjusts the power delivered to the load regarding the battery SOC (State-Of-Charge). The proposal has been included in a simulated wireless charger operating at 85 kHz, which corresponds to the operational frequency recommended by SAE 2954 [6]. The simulations results show the ability of

the proposed wireless charger to adapt to diverse battery states.

The remainder of the paper is structured as follows. Section II includes the details of the design of the proposed wireless charger, paying special attention to the PFC. Section III presents the results of evaluating the performance of the PFC. Finally, Section IV draws the main conclusions of our work.

II. Power-Factor Corrector Design

A. Schemes

The scheme of the proposed wireless charger is depicted in Fig. 1. In the primary side, the grid source is connected to an AC/DC rectifier which includes a PFC. Then, a DC-DC converter sets the voltage to the requirements imposed by the full-bridge inverter. The inverter output is connected to a capacitor which is in series with the primary coil. On the other hand, the secondary coil counts also with a series compensation and a HF rectifier. A DC-DC converter may be employed in the secondary side to adapt the rectifier output to the battery features.

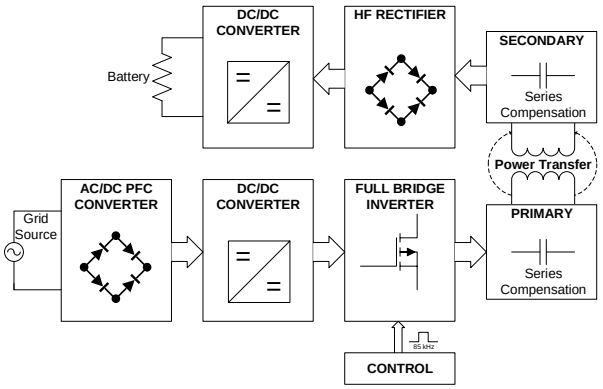

Fig. 1. Wireless charger scheme.

The designed wireless charger is equipped with two isolated control algorithms: one placed in the PFC and another in the inverter. The goal of the inverter control is to maintain a fixed voltage in the battery for different SOC, that is, when its equivalent model corresponds to a variable resistance. Towards this goal, a square-wave control with dead times is used in the inverter. The length of the dead intervals is tuned to properly set the gating signals of the full-bridge inverter. This length is dependent of the load features so that the power delivered by the source can be modified accordingly to the battery states. More details about this adjustment may be found in [7].

The PFC control does not require the execution of any control in the inverter. Nevertheless, the switching strategy strongly impacts on the input harmonics so that inverter control schemes clearly benefits from the inclusion of a PFC.

The proposed PFC is shown in Fig. 2.An ACC (Average Current-Mode Control) strategy is used as it simplifies the design of EMI (ElectroMagnetic Interference) filters and it also reduces the impact of zero crossings. Basically, the control adjusts the duty cycle of PFC switching signal by attending at two feedback loops: a slow-response voltage regulator and a faster current regulator.

To decide the duty cycle, the PFC control exclusively employs electrical measurements derived in the same power converter. Specifically, it requires the PFC output voltage (V_o), the PFC input voltage (V_g), the current traversing the PFC coil (ILf) and a voltage reference (V_{ref}). The voltage reference is set to 400 V. This voltage level is the maximum needed in order to reach the power requirements of the complete wireless charger. In particular, a 3.7 kW wireless charger is considered. In addition, a boost DC/DC converter stabilizes the inverter input voltage.

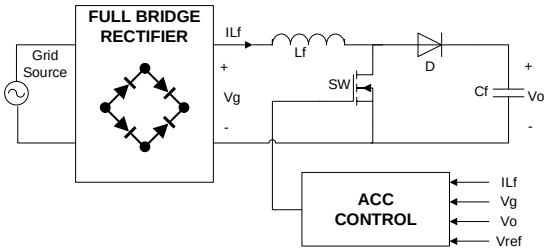

Fig. 2. PFC Scheme

B. PFC Control

The designed PFC corresponds to a boost converter enhanced with a control system. The structure of the control system is reflected in Fig. 3.

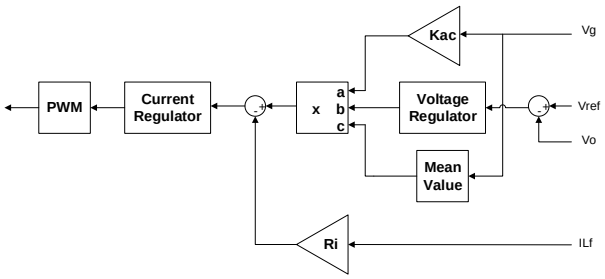

Fig. 3. Structure of the PFC control.

Inductor current (I_{Lf}) is sensed and amplifies by the gain R_i. Then, it is compared with the signal obtained from a multiplier. This multiplier takes into account:

1. V_g waveform amplified by the gain K_{ac}.
2. V_g mean value.
3. The external voltage regulator.

As a result of the comparison, the internal current is set up. The internal loop is governed by the transfer function $G_i(s)$.On the other hand, the output voltage (V_o) and a voltage reference (V_{ref}) are compared to feed the voltage regulator, with a transfer function referred as $G_v(s)$.

As can be observed, there are two control loops. These loops are:

- Current loop. The main goal is that the inductor current is in phase with the rectified grid voltage. To do so, *Gi(s)* is configured to work with a cutoff frequency greater than ten times the grid fundamental harmonic (50 Hz). A value of 800 Hz is selected in our proposal, but a higher frequency is also possible.
- Voltage loop. It is responsible for setting up the output voltage level. Its bandwidth must be lower than the grid frequency in order to reduce the harmonic distortion. Conversely, it should be as high as possible to ensure adequate system's dynamics. Generally, 10 times lower than grid frequency is enough.

Finally, the signal provided by the current regulator is compared with a saw-tooth waveform at 65 kHz. A Pulse-Width Modulation technique is then used so that the duty cycle varies according to the current regulator output.

C. PFC design

In this Subsection, we describe how the components of the PFC are selected. As previously mentioned, a single-phase wireless is considered so that the maximum output power (P_o) is assumed to be 4000 kW. Firstly, we justify how the appropriate coil's inductance is chosen.

The maximum peak inductor current (I_{coil}) occurs when the input is the lowest one, which is referred as Vac_{LL}. For the DC-DC converter employed, the relationship between these two magnitudes is expressed as follows:

$$I_{coil,(\max)} = \frac{\sqrt{2}P_o}{\eta \cdot Vac_{LL}} \tag{1}$$

being η the system efficiency. For our particular configuration, the peak current is 64.93 A. In addition, it is recommended to choose a current ripple between 25-45%. There is no inductance value equation for the Current-Control Mode PFC. However, an approximation of the coil inductance can be obtained with the following equation [8]:

$$Lf = \frac{Vac_{LL}^2}{2 \cdot CR \cdot f_{sw} \cdot P_o \cdot \eta}\left[1 - \left(\frac{\sqrt{2}Vac_{LL}}{V_o}\right)\right] \tag{2}$$

where f_{sw} is the switching frequency. For our particular case, the obtained autoinductance is 43.35 µH.

Concerning the switch, a MOSFET has been selected in order to cope with the frequent switchings. To determine the specific MOSFET required by our application, we need to take into account the PFC output voltage and the RMS current traversing the transistor (I_m). The current traversing the transistor is expressed as follows:

$$I_{M(RMS)} = \frac{P_o}{Vac_{LL} \cdot \eta}\sqrt{1 - \frac{8\sqrt{2} \cdot Vac_{LL}}{3\pi V_o}} \tag{3}$$

Conduction losses depend on the previously computed current and on the resistance drain-source $R_{ds(on)}$, so a low value in this parameter is a must. Therefore, attending at output voltage and current, a MOSFET component SK60MH60 is chosen. The losses associated to this component applied to our configuration are computed next in order to determine the need for heatsink. Firstly, we model the power losses when the MOSFET is activated (P_{on})

$$P_{on} = I_{M(RMS)}^2 \cdot R_{ds(on)} \tag{4}$$

This active power is equal to 111.66 W. Nevertheless, more phenomena need to be considered. Particularly, switching losses also impact on the consumed power. One of the most significant contributions on this metric is the capacitive turn-on losses (P_{sw}) . This member is computed according to the following Equation:

$$P_{sw} = \frac{2}{3} \cdot Coss_{25} \cdot \sqrt{25} \cdot V_{on}^{1.5} \cdot f \tag{5}$$

where $Coss_{25}$ corresponds to the output capacitance under the following conditions specified in the datasheet: $V_{DS} = 25\,V$, $V_{GS} = 0\,V$ and frequency $f = 1\,MHz$. V_{on} is the output voltage. P_{sw} is equal to 10.67 W. The selected MOSFET is able to cope with the computed power.

On the other hand, the diode is selected basing on the power that it supports when it is operating in the active region (P_{on}). This power is computed as follows:

$$P_{ON} = I_d \cdot V_T = \frac{P_o}{V_o}V_F = 23.90\,W \tag{6}$$

where V_F is the Forward voltage. For our application, the diode consumes 23.90 W. The diode LXA20T600 is able to dissipate this power and it also allows 600 V when it is not conducting. This component is modeled with a V_F equal to 2.3 V.

Finally, when determining the capacitor to employ, the following parameters need to be taken into account: the voltage ripple (V_{ripple}), the output capacitor current (I_{Co}) and the hold-up time (t_{hu}). These electrical magnitudes are characterized by the following equations:

$$V_{ripple} = \frac{P_o}{2\pi f_{sw} C V_o} \tag{7}$$

$$I_{Co(rms)} = \sqrt{\frac{32\sqrt{2} \cdot P_o^2}{9\pi Vac_{LL} \cdot V_o \cdot \eta^2} - \left(\frac{P_o}{V_o}\right)^2} \tag{8}$$

$$t_{hu} = \frac{C(V_o^2 - V_{min}^2)}{2P_o} \tag{9}$$

where P_o and V_o are output power and voltage, η is the converter efficiency and Vac_{LL} is the lower input voltage allowed.

A capacitor of $C = 2 \cdot 5.6\, mF$ leads to $V_{ripple(pp)} = 2.95\, V$, $I_{Co(rms)} = 25.75\, A$ and $t_{hold-up} = 55.05\, ms$. These results are acceptable for the application under study as less than 1% output voltage ripple and a hold-up time higher than two source periods are reached [8].

III. Performance Evaluation

The benefits of incorporating a PFC are evaluated by means of a Simulink model of a wireless charger [9]. The main features of the wireless charger are summarized in Table I.

TABLE I. WIRELESS CHARGER'S MAIN FEATURES

Parameter	Wireless Charger's Main Features		
	Description	***Value***	***Unit***
M	Mutual inductance	40.8017	µH
C_1	Primary compensation capacitor	12.1590	nF
C_2	Secondary compensation capacitor	12.9785	nF
L_1	Primary coil inductance	288.3390	µH
L_2	Secondary coil inductance	270.1323	µH
R_{L1}	Primary coil equivalent resistor	30.8950	mΩ
R_{L2}	Secondary coil equivalent resistor	27.7839	mΩ
R_L	Battery resistor	24.3243	Ω
$G_{DC\text{-}DC}$	Gain in the Primary DC-DC converter	0.75	
f_0	Operating frecuency	85	kHz
P_L	Output power	3700	W
V_L	Output voltage	300	V

When a PFC is not included in the system, current provided by the utility presents severe harmonic distortion. In fact, the frequent switchings occurred in the power converters are responsible for originating a non-senoidal current signal. These two magnitudes are depicted in Fig. 4.

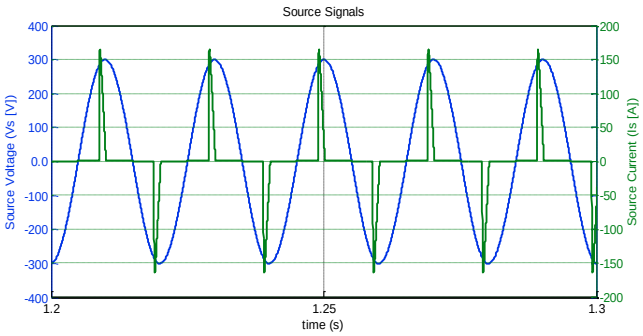

Fig. 4. Source Voltage and Source Current when the PFC is omitted.

By means of a Fourier analysis, we can derive the power factor (*PF*) perceived by the source. Particularly, for our experiments when the load can be modeled as a resistance equivalent to 24.3243 **Ω**, the obtained *PF* is 0.4429. Alternatively, when the SOC of the battery varies and, as a consequence, the load is approximated to 48.6486 **Ω**, then the *PF* is 0.3860.

The evaluation concerning the PFC has been carried out with two goals. Firstly, we wanted to analyze the capability of the proposed scheme to improve the system efficiency, as it was the main requirement. Nevertheless, we also study how the PFC is able to operate for different battery states. Specifically, an abrupt change is triggered at 1.75 s to modify the value associated to the load resistance from 24.3243 **Ω** in its nominal operation point to 48.6486 **Ω**. The mean value of the PFC is shown in Fig. 5.

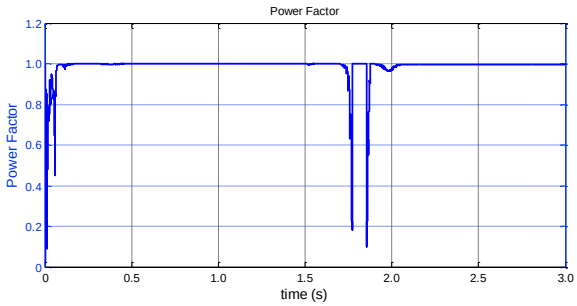

Fig. 5. Resulting PF when the proposed scheme is implemented.

Although the proposed PFC scheme needs about 0.25 s to stabilize its behavior, the simulation results show that the PFC control works properly as it adapts the current waveform in order to increase the power factor. In turn, the system efficiency is also improved. In particular, there is a significant increment in the system efficiency from 0.4429 to 0.9996 when the load resistance corresponds to its nominal value. When the battery's features vary, the system efficiency is also maintained to 0.9961, which is a clear benefit from the scenario where the PFC is not incorporated and which leads to an efficiency equal to 0.3860.

IV. Conclusions

Frequency conversion required by wireless chargers imposes the generation of multiple current harmonics, which may noticeably deteriorate the system efficiency. In order to overcome this significant limitation, PFC techniques need to be incorporated. This paper has presented a PFC which does not need any feedback signals from the secondary to operate even when it adapts its behavior to different battery states. An average current control method is used. The simulation results show how the power factor perceived by the utility is corrected for different battery states.

As a future work, the authors will physically implement the proposed wireless charger and they will evaluate the potential deviation of the obtained results from the theoretical ones.

REFERENCES

[1] F.Musavi, W. Eberle, "Overview of wireless power transfer technologies for electric vehicle battery charging," *IET Power Electronics*, vol.7, no.1, pp.60,66, January 2014

[2] S.Y.R.Hui, Zhong Wenxing, C.K. Lee, "A Critical Review of Recent Progress in Mid-Range Wireless Power Transfer," *IEEE Transactions on Power Electronics*, vol.29, no.9, pp.4500,4511, Sept. 2014

[3] K. Jezernik, "Power control strategy for unity power factor," *2010 IEEE International Symposium on Industrial Electronics (ISIE)*, 4-7 July 2010

[4] M.G.Egan, D.L. O'Sullivan, J.G.Hayes, M.J. Willers, Christopher P.Henze, "Power-Factor-Corrected Single-Stage Inductive Charger for Electric Vehicle Batteries," *IEEE Transactions on Industrial Electronics*, vol.54, no.2, pp.1217,1226, April 2007

[5] Liang-Rui Chen; Hai-Wen Chang; Chia-Hsuan Wu; Chung-Ming Young; Neng-Yi Chu, "Voltage controllable power factor corrector based inductive coupling power transfer system," *2012 IEEE International Symposium on Industrial Electronics (ISIE)*, pp. 582,587, 28-31 May 2012

[6] SAE International, www.sae.org

[7] A. Triviño-Cabrera, M. Ochoa, D. Fernández, J. A. Aguado, "Independent Primary-Side Controller applied to Wireless Chargers for Electric Vehicles", IEEE-IEVC2014

[8] "Power Factor Correction Handbook". Rev. 4, ON Semiconductor, 2011.

[9] Simulink. www.mathworks.com